VASIMR® VX-200 Operation at 200 kW and Plume Measurements: Future Plans and an ISS EP Test Platform

IEPC-2011-154

Presented at the 32nd International Electric Propulsion Conference,
Wiesbaden • Germany
September 11 – 15, 2011

Jared P. Squire[1], Chris S. Olsen[2], Franklin R. Chang Díaz[3], Leonard D. Cassady[4], Benjamin W. Longmier[5], Maxwell G. Ballenger[6], Mark D. Carter[7], Tim W. Glover[8] and Greg E. McCaskill[9]
Ad Astra Rocket Company, Webster, Texas, 77598, USA

Edgar A. Bering, III[10]
University of Houston, Houston, Texas, 77204, USA

The VASIMR® VX-200 experimental device has been fully operational at 200 kW for nearly 2 years. Many improvements to the experimental configuration, since last reported, have enabled high fidelity performance measurements and detailed plume characterization up to 2.4 m downstream of the thruster. Rapid plasma start up (< 100 ms) and automated high vacuum systems were critical for achieving measurements with the charge exchange mean-free-path approximately 1 to 2 m in the background neutral gas. The thruster performance at 200 kW is 72 ± 9%, the ratio of effective jet power to input RF power, with an I_{sp} = 4900 ± 300 seconds. The thrust increases steadily with power to 5.8 ± 0.4 N until the power is maximized and there is no indication of saturation. Comparisons of the plasma flux to magnetic flux in the plume show evidence that the plasma flow does not follow the magnetic field at distances downstream on the order of 2 m. The plume is more directed when the ions are significantly accelerated. The primary future effort for the VX-200 project is to install components and systems to enable steady state operation. A proposed Electric Propulsion and Power Platform is introduced for testing VASIMR® and other high power devices in the space environment onboard the International Space Station (ISS). It features a high energy storage, 50 kW-hr, battery to utilize the available power on the ISS and test at 200 kW for 15 minutes. The ISS provides human access and potential replacement and inspection of test components as in a laboratory.

Nomenclature

I_{sp} = specific impulse [s]
α = specific mass [kg/kw]
η = rocket efficiency, jet power/DC power

[1] Sr. VP of Research, jared.squire@adastrarocket.com.
[2] Research Scientist, chris.olsen@adastrarocket.com.
[3] President and CEO, aarcinfo@adastrarocket.com.
[4] Senior Aerospace Engineer, lcassady@adastrarocket.com.
[5] Principal Research Scientist, ben.longmier@adastrarocket.com.
[6] Staff Scientist, maxwell.ballenger@adastrarocket.com.
[7] Director of Technology, mark.carter@adastrarocket.com.
[8] Sr. VP of Development, tim.glover@adastrarocket.com.
[9] Senior Electrical Engineer, greg.mac@adastrarocket.com.
[10] Professor, Physics, eabering@uh.edu.

e = electron charge [C]
f_i = ion flux plume fraction
f_Φ = magnetic flux plume fraction
J_{iz} = axial current density [A/m^2]
Γ_{iz} = axial ion flux [ions/s]
Φ_B = axial magnetic flux [Wb]
B_z = axial magnetic flux density [G]
r_{edge} = projected magnetic plasma boundary [m]
ρ = mass density [kg/m^3]
u = ion velocity [m/s]
S = External ionization sources [ions/s/m^2]
L = External ionization losses [ions/s/m^2]

I. Introduction

THE VASIMR® engine[1,2] technology is inherently a high power (> 100 kW) system. A key distinguishing feature from other high power electric propulsion (EP) devices is that the plasma stream, both ions and electrons, inside of the rocket is highly magnetized. The ion gyroradii are much smaller than the plasma radius. This enables strong radial confinement and efficient coupling of high power density (> 1MW/m^2) radio frequency (RF) power. Therefore, a prominent component of the engine is a superconducting magnet that produces a properly shaped magnetic field profile. VASIMR® does not scale down in power well, since the magnet then becomes a large mass overhead. The very high power density (> 5 MW/m^2) capability of the efficient RF driven plasma stream at high power makes the system an attractive performer ($\alpha < 10$ *kg/kW* and $\eta > 0.6$).

Figure 1 shows a diagram of the major components of the rocket engine. It has two independently powered stages, one to produce dense plasma and the other to accelerate the flow. The first stage is a high power helicon[3,4] plasma source and the second is based on single pass ion cyclotron heating (ICH).[5] The helicon is a proven high efficiency plasma source for this application.[6,7] The ICH acceleration process in this configuration is a proven efficient means to produce an energetic flowing dense plasma jet.[8,9] Controlling the ratio of power in the two stages, together with optimizing the propellant injection rate, gives I_{sp} throttling.

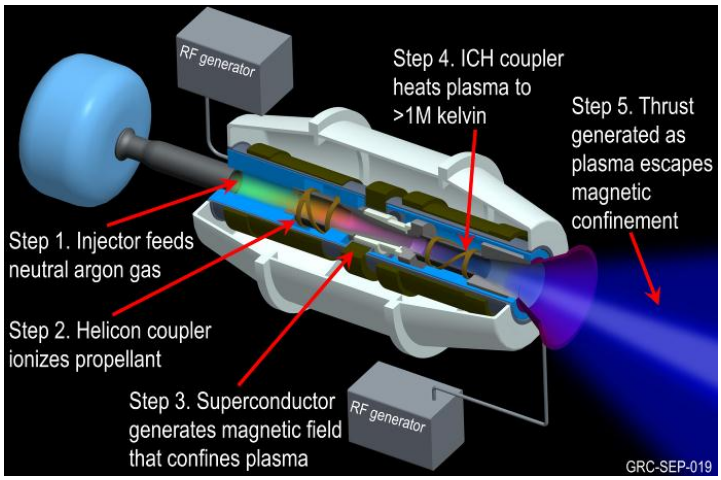

Figure 1. Schematic of the VASIMR technology elements.

This paper presents recent rocket performance results at up to 200 kW of RF power in the VX-200 experimental device. At an RF power level of 100 kW, we present detailed plume measurement data and address the plasma flow as compared to the expanding magnetic field, showing detachment. Future plans for this work are discussed. Finally, we briefly describe a proposed Electric Propulsion and Power Platform, named *Aurora*, for testing of VASIMR® and other high power devices onboard the International Space Station.

II. Test Configuration

The VASIMR® VX-200 experimental 200 kW device and test facility have been fully operational for nearly two years and have been previously described.[10,11] We will summarize the configuration here and note recent improvements.

A. VX-200

The VX-200 is a cryogen-free superconducting device with a peak magnetic field strength of 2 T. The system is designed for >200 kW DC input power operation. The RF power is generated from two high efficiency solid-state generators with a combined conversion (DC to RF) efficiency of 95%. The impedance matching circuits couple 98% of the RF power to the plasma. Argon propellant is regulated into the first stage using a Moog proportional

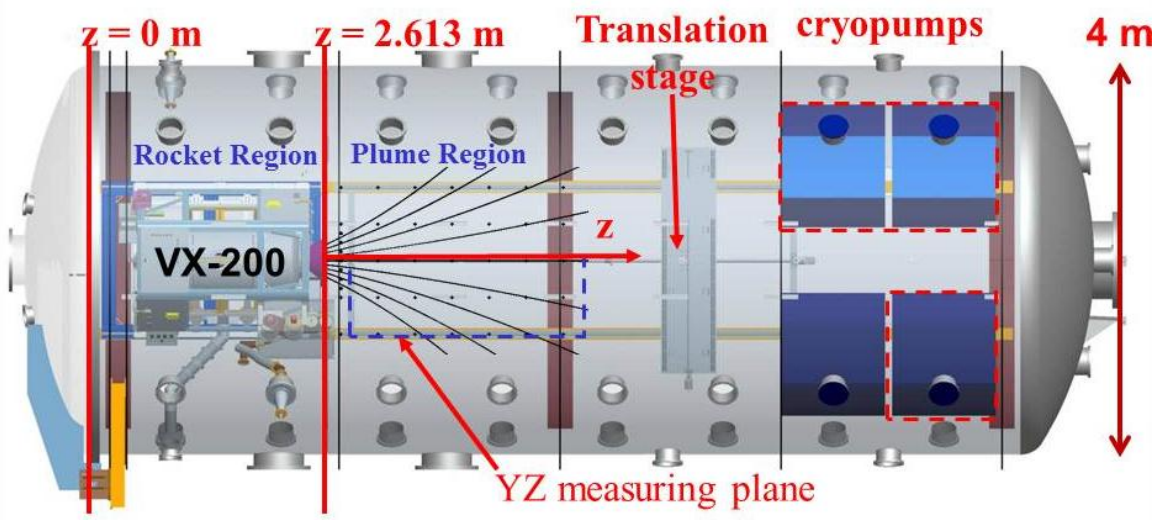

Figure 2. VX-200 installed in the vacuum chamber with translation stage and coordinate system noted. The reference for z = 0 m is the large end flange of the chamber and the last physical structure attached to the rocket ends at z = 2.613 m.

flow control valve (PFCV) capable of up to 150 mg/s. The plasma output diameter is approximately 0.2 m at the location where the energetic ion population in the expanding magnetic field has converted most of its velocity (~ 90%) to directed axial motion. Most VX-200 pulses are between 1 and 15 seconds in length, due to thermal and vacuum limitations. Figure 2 depicts the VX-200 installed in the vacuum chamber.

The first stage, or helicon stage, launches a right-hand circularly polarized wave into the plasma. The plasma diameter is reduced by more than a factor of 2 as it flows downstream through a "magnetic choke" and gas containment wall that follows the plasma flux tube. The second stage of the rocket, the RF booster, or Ion Cyclotron Heating (ICH) stage, deposits energy directly into the ions via an ion cyclotron resonance interaction with an ion cyclotron wave[12] that is launched from the high magnetic field side of the resonance by a proprietary coupling structure.

The VX-200 utilizes two solid-state RF generators developed by Nautel Ltd. of Canada specifically for this application. The helicon section RF generator converts power supplied at 375 VDC into approximately the industrial standard of 6.78 MHz RF with an efficiency of 91±1% at up to 48 kW and weighs 40.1 kg without the enclosure. The ICH section RF generator converts power supplied at 375 VDC into approximately 500 kHz RF with an efficiency of 98±1% at up to 180 kW and weighs 87.1 kg without the enclosure. RF power is transmitted into the vacuum chamber through high-power RF feedthroughs and into capacitor networks mounted on the VX-200 that transform the impedance for efficient coupling to the plasma load.

Since previously reported[10] in 2009, many improvements have been made in the operation of VX-200, including RF control for rapid start-up, instrument upgrades and vacuum facility upgrades. The RF tuning has been optimized, together with FPGA timing, to achieve highly repeatable plasma fast start-up (<100 ms) to over 35 kW of regulated power in the first stage. The vacuum facility, with a new bulk 24,000 liter bulk LN_2 tank, has automated operation of three of the four installed cryopanels with 150,000 l/s pumping rate for these data. This has generated a large body of data and experience with running such a high power device.

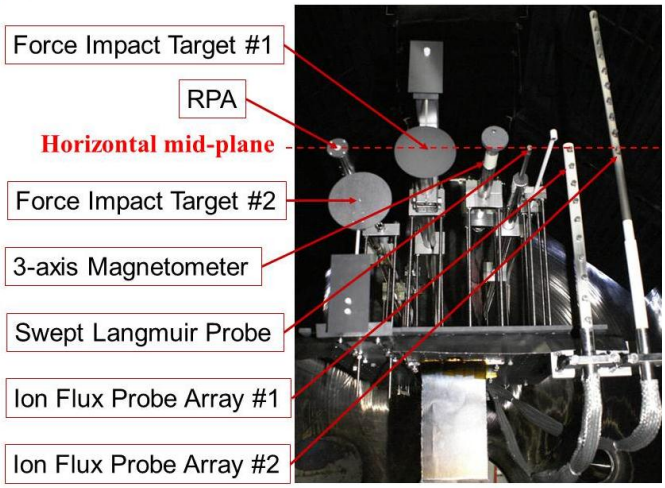

Figure 3. The platform on the translation stage showing the plasma diagnostics installation.

B. Measurements

There is a 2.5 m by 5 m translation stage with a positional resolution of 0.5 mm that carries a suite of plasma diagnostics for plume characterization on

the horizontal plane (Fig. 3). We use a right handed coordinate system with the z-axis pointing downstream and the x-axis pointing up. Plasma flux measurements are performed using two planar molybdenum 10-collector Langmuir probe arrays biased into ion saturation and mounted on the translation stage so that they collect vertical profiles both 0.3 m above and below the horizontal plane. To determine a quantity for thrust, we rely on a force target (plasma momentum flux sensor) technique that has been validated against a Hall thruster on a thrust stand.[13] The force target is a graphite disk mounted to a sensitive strain gauge and scanned across the plasma profile to integrate a total force that we interpret as thrust. The plume data presented in this paper results primarily from the Langmuir probe array. There is also a swept planar Langmuir probe mounted near the probe array facing into the flow. A three axis magnetometer is placed behind a graphite disc for protection from the intense ion flow. The method of measuring thruster performance is described in more detail elsewhere[14] and further discussed in an accompanying paper.[15]

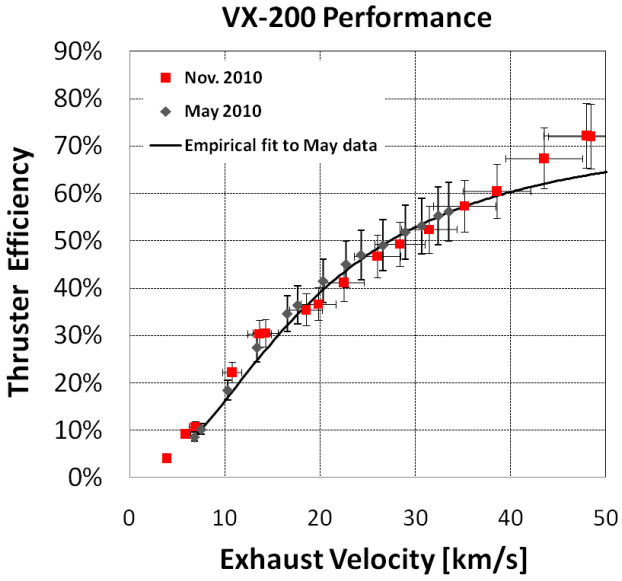

Figure 4. Thruster efficiency plotted verses exhaust velocity for two different test runs with a semi-empirical model fit to the May data.

III. Performance at high power

Recently, the work has led to a measurement of thruster performance at the full 200 kW RF power level and in a vacuum environment (< 10^{-5} torr) where effects due to background neutral interactions are minimal. Figure 4 shows the primary result of thruster efficiency versus effective exhaust velocity. Another paper[14] describes details regarding the data from May 2010. In the graph, we fit the May data with a semi-empirical model[14] and extrapolate that fit from an exhaust velocity of 33 km/s to 50 km/s, corresponding to 112 kW and about 200 kW total RF power, respectively. The thruster efficiency is defined by the jet power, as measured by the input gas flow rate and integrated force target data, divided by the input RF power, as measured at the RF generator output.

This power scan was accomplished by fixing the helicon power at 30 kW and adding an ICH power ramp up to 170 kW. A gas flow temporal profile was required to achieve the high power ramp while maintaining proper impedance matching. The efficiency data points for less than the highest power were acquired during the power ramp, so are not optimized. These data show that the ICH stage is very effective at accelerating ions with efficiency, defined as the coupled ICH power to ion kinetic energy, of 82%. The acceleration process shows no signs of saturation, as exhibited in figure 5, since the measured force increases almost linearly until we maximized the available power. Through this scan, the propellant utilization was near 100%, although only the highest power point was optimized for gas flow. The ionization cost is less than or about 100 eV/ion[7, 15] for the helicon alone and we are preparing an effort to study this quantity with ICH power applied. We expect that the lower power points will increase efficiency when we optimize the gas flow for each power setting of the two stages. Nevertheless, the thruster efficiency with argon gas exceeds 50% for I_{sp} above 3000 seconds

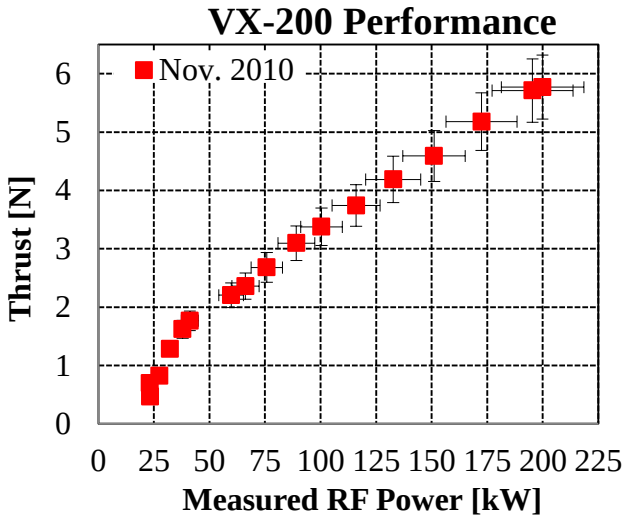

Figure 5. Thrust verses input RF power.

and reaches a value of 72 ± 9%, exceeding the extrapolated value near 5000 seconds. The plasma power density at the rocket exit is approximately 5 MW/m^2, where graphite of the force target glows red hot.

IV. Plume measurements

Improved VX-200 control algorithms and synchronization along with vacuum facility upgrades have enabled detailed exhaust plume studies with minimal charge exchange interaction (λ_{mfp} > 1 m). In the latest campaign, measurements were performed during total RF power levels of 30 kW (helicon only) and 100 kW (70 kW ICH added), corresponding to each stage of the engine, throughout a volume extending 2.4 m downstream from the last physical structure that is attached to the rocket. Plasma parameter maps, such as ion flux, particle momentum flux, parallel ion energy, magnetic field, electron temperature, and plasma potential, were taken shot-to-shot on a regular grid using more than 450 highly repeatable shots. Figure 6 displays the RF power level, propellant flow rates, and chamber pressure with uncertainty bounds.

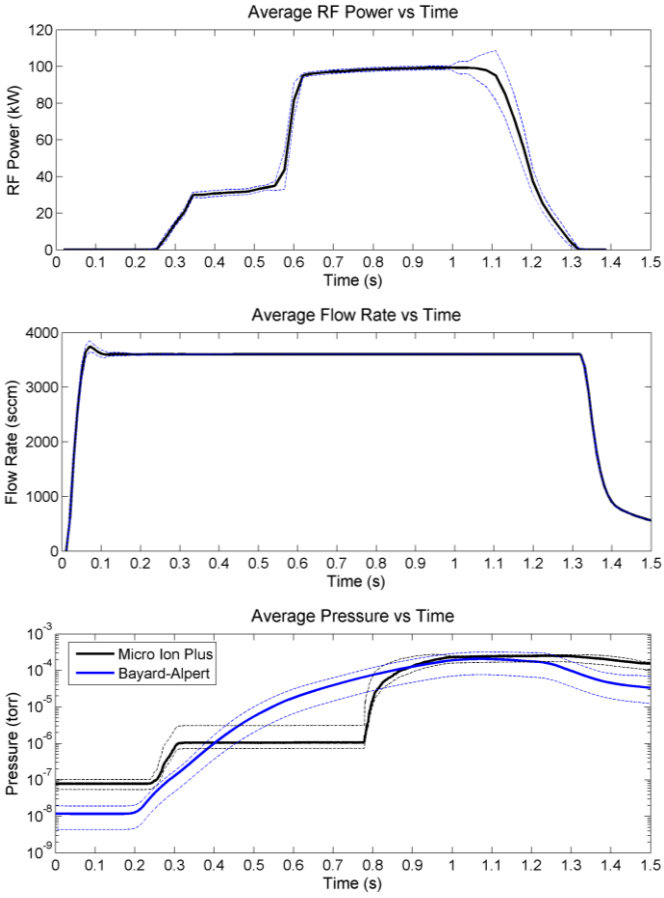

Figure 6. Standard shot configuration for the plume study with uncertainty bounds (dashed lines). Data analysis time windows for low and high power configurations were taken from 0.4-0.5 s and 0.65-0.75 s respectively. (*Top*) Average RF forward power profile. (*middle*) Steady 100 mg/s (3600 sccm) argon flow. (*bottom*) Exhaust region chamber pressure measured by independent ion gauges.

One of the main purposes of this recent study is to experimentally demonstrate that the plasma flow has separated from the magnetic field in this downstream region of the VX-200 plume. Previous attempts have been made comparing a single measured plume radius to simulation[16] as well as using different propellants and plasma source while comparing to a simplified magnetic field scaling.[17] We present an alternative method, under improved conditions, to verify that the flow detaches from the magnetic field in which we compare the spatially integrated axial ion flux and magnetic flux in the magnetic nozzle region of the exhaust plume. We begin by taking the continuity equation and making the assumption that charge sources and losses in the plume are negligible, and that the flow is steady state.

$$\frac{\partial \rho}{\partial t} + \nabla \cdot (\rho \vec{u}) = S - L \approx 0 \qquad (1)$$

This permits the measurement of the plasma/magnetic flux expansion within the magnetic nozzle without worry of external influences. The ion flux probes are planar probes which restricts us to compare only the axial components of particle and magnetic flux. A baseline flux is established using data from a diameter scan at an axial position closest to the rocket exit. The ion flux is integrated radially outward from the peak of the plume to r_{edge}, a position determined by a projection of the magnetic field from the edge of the rocket core. Azimuthal symmetry about the peak of the plume/magnetic field is assumed.

$$\Gamma_{iz}(r) = 2\pi \int_{r_{peak}}^{r} \frac{J_{iz}}{e} r dr \qquad (2)$$

$$f_i(r) = \frac{\Gamma_{iz}(r)}{\Gamma_{iz}(r_{edge})} \tag{3}$$

$$\Phi_z(\mathrm{r}) = 2\pi \int_{\mathrm{r}_{peak}}^{r} B_z r dr \tag{4}$$

$$f_\Phi(r) = \frac{\Phi_z(r)}{\Phi_z(r_{edge})} \tag{5}$$

Equations 2 and 3 describe the radial particle flux integration and ion plume fraction, f_i, which are used to map lines of constant ion flux in the magnetic nozzle region. Equations 4 and 5 are similar to 2 and 3 in that they describe the radial integration of magnetic flux and are used to map lines of constant *enclosed* magnetic flux. Figure 7 shows a diagram of this concept comparing fluxes as a function of spatial position. The ions may be considered detached so long as they do not expand at the same rate as the enclosed magnetic flux.

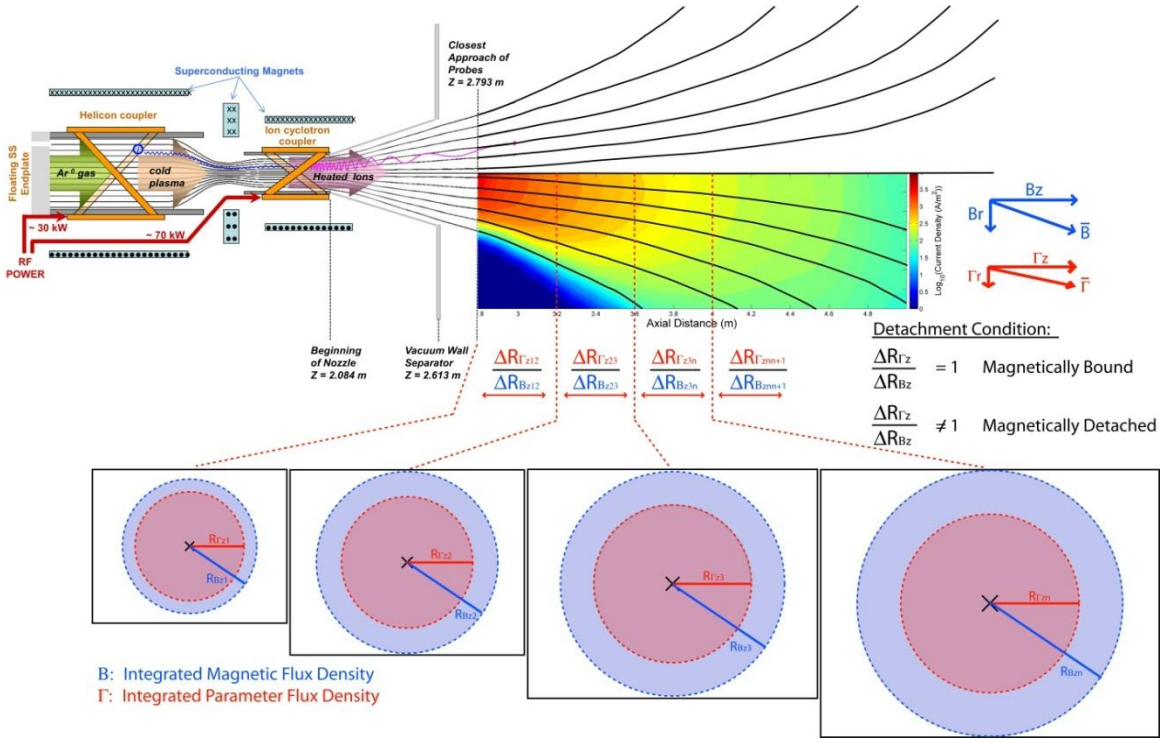

Figure 7. Experimental determination of ion detachment in the plume of the VX-200. Lines of constant ion flux and magnetic flux are tracked spatially throughout a majority of the magnetic nozzle region. Comparing the rate of expansion gives a verification of the directionality of the plasma plume and a rough idea of the nozzle efficiency.

For each remaining axial z position the fluxes were integrated radially outward until the flux matched discreet values of the plume fraction (f_i, f_Φ = 0.1, 0.3, 0.5, 0.7, and 0.9). Figure 8 plots ion flux contours with an overlay corresponding to the r, z locations of the integrated ion flux and magnetic flux for the 50% plume fraction. Error bars take into account systematic uncertainties as well as hardware resolution. It is clear that the ion flux does not follow the magnetic flux in either the low power (Figure 8, top) or the high power configurations (Figure 8, bottom). In this magnetic nozzle region the lower energy ions appear to diffuse radially outward while the higher energy ions form a more axially directed flow (Figure 9). The radial diffusion of the momentum flux directly affects the efficiency of the magnetic nozzle. The mechanisms in the nozzle region governing the plasma flow are still under investigation. The data here represent a subset of a much larger dataset and analysis is still on-going.

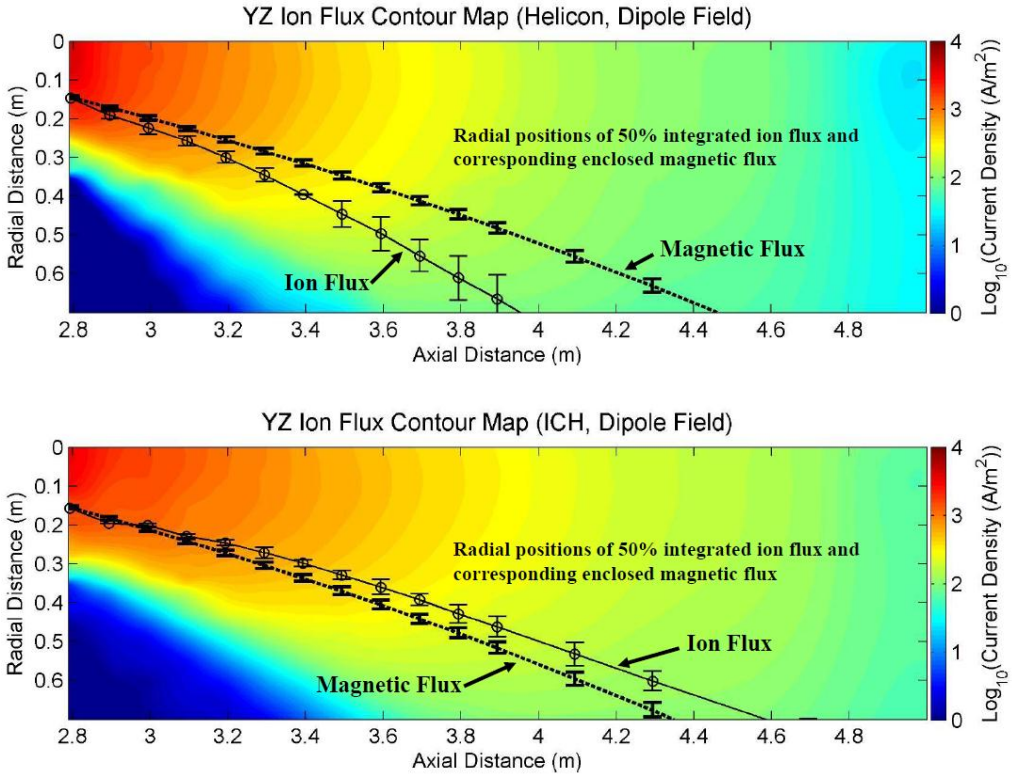

Figure 8. Ion flux color contour maps in the magnetic nozzle region of the plume. Lines of constant axial ion flux (solid line w/ open circles) and magnetic flux (dashed line) are overlain, 50% plume fraction in this case. The ion flux in either case does not follow the magnetic flux. (*top*) The low power configuration (helicon only ~ 30 kW) shows the ion flux diverging faster than the enclosed upstream magnetic flux. (*bottom*) The high power with ICH (total RF power ~ 100 kW) ion flux forms a more directed flow resulting in a higher nozzle efficiency.

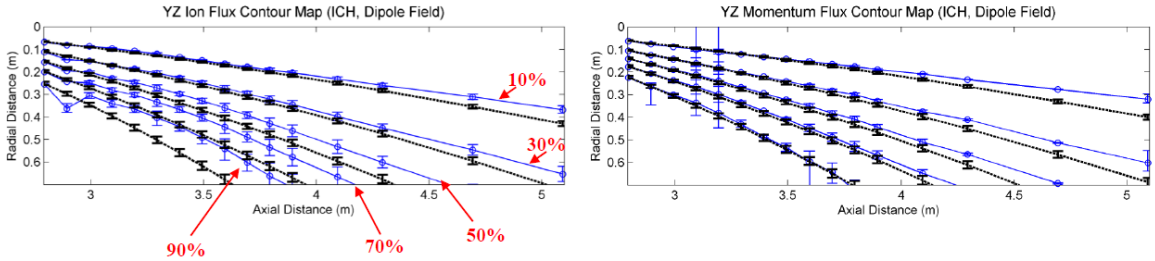

Figure 9. Comparison of radially integrated ion/momentum (solid blue lines) and magnetic (dashed lines) fluxes for the 10%, 30%, 50%, 70%, and 90% plume fractions. The high power configuration (total RF power ~ 100 kW) is shown here. The ion flux and momentum flux in all plume fractions are shown to be directed more axially than the magnetic flux resulting in higher nozzle efficiency than under helicon alone. (*left*) High power ion flux. (*right*) High power momentum flux.

V. Future Plans

VX-200 operations are presently limited to less than 1 minute pulses because the first generation device does not implement high power active cooling and has temperature limited seals. Our first goals were to demonstrate the RF power and plasma flow function, while measuring heat loads and thruster performance, which are all established within 10 s. These goals have been accomplished. We are in the process of refining detailed heat flux measurements using an IR camera and IR sensors. Engineering efforts are underway to modify VX-200 for full

steady-state capability. This requires high temperature ceramics with seals that are compatible with the RF environment. We also have the challenge of transporting the heat from the magnet bore and coupling it into a rejection system.

Facility challenges to withstand a 150 kW plasma exhaust jet are significant. We are designing and installing an improved vacuum chamber divider wall to better seal against neutral pressure back flow to the VX-200 vacuum section and withstand stray heat. A plasma beam dump with heat rejection will intercept most of the jet power downstream at distance of roughly 5 m, so the plume can still be characterized over this space. We are upgrading plasma diagnostics with graphite and ceramics to withstand the intense environment. Such steady-state operations will require additional pumping by installing more cryopanels. The vacuum facility is capable of bringing the count to 16 panels and a total pumping speed exceeding 1,000,000 l/s (N_2); although, initial modifications may include 8 panels. The section upstream of the divider wall will also require more pumping as components become hot and outgassing rates from the VX-200 engine increase.

This will enable lifetime and erosion measurements with hundreds of hours of operation at full power density. The modification work is planned for the coming year with long duration tests to follow soon thereafter. First stage lifetime studies are in progress at our facility in Liberia, Costa Rica and are discussed in an accompanying paper.[18]

Refinement of RF control techniques and impedance matching are underway. Detailed measurements of the RF temporal behavior of the complex impedance (resistive and reactive) enable the development of control algorithms for the operational parameter space. This information also provides a basis for impedance matching power circuit design that optimally and robustly couples power from the RF generators to the plasma.

VI. ISS EP Test Platform

Ad Astra Rocket Company is in the process of defining specifications for and designing an Electric Propulsion and Power Test Platform, named *Aurora*, for installation on the International Space Station (ISS), shown in figure 10. Its primary purpose is to demonstrate the operation of a VASIMR® 200 kW engine (VF-200) in the space environment. Since the ISS is power limited, the Aurora platform plans to include a 50 kW·hr battery to supply 200 kW of power for up to 15 minutes (sufficient to significantly heat VF-200 thermal management systems) and trickle charge from ISS power between firings. Aurora and VF-200 offer unique opportunities to study the flow of the plasma in a 3-d magnetic field geometry without the effects of conducting boundaries. Additionally, high power and infrastructure may be made available for testing other high power devices in the space environment with the human-tended access offered by the ISS. An interface is planned, potentially FRAM (Flight Releasable Attach Mechanism) based, located on top of the structure with a zenith view. The site could feature power and data interfaces for a variety of potential test payloads. Payloads could be robotically installed and exchanged.

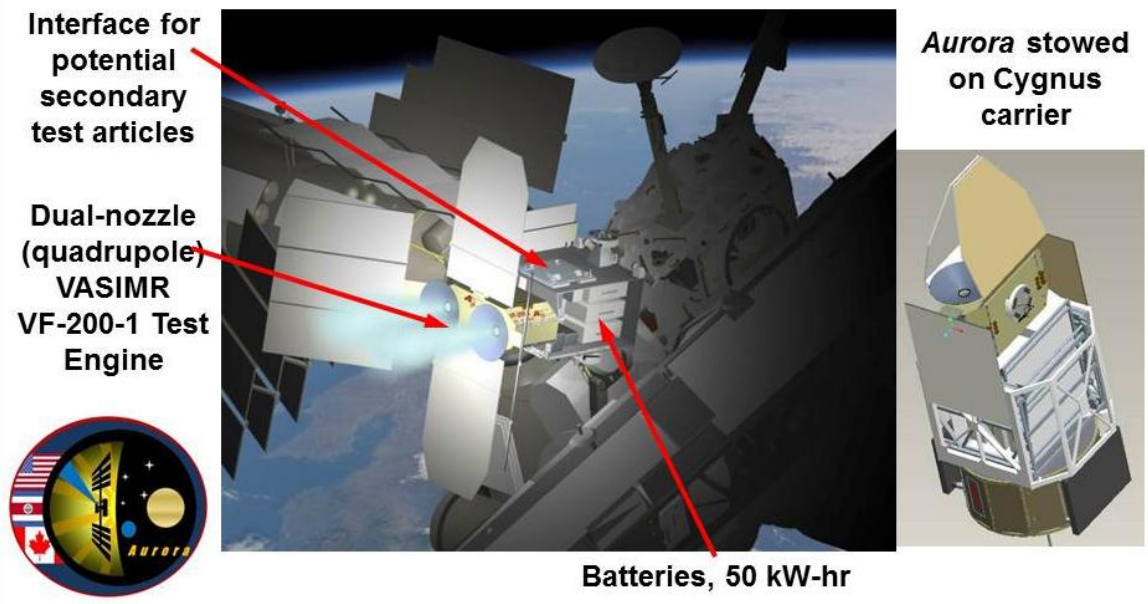

Figure 10. The Aurora Electric Propulsion and Power platform installed on the ISS and packaged on a Cygnus transfer vehicle.

VII. Conclusion

We have summarized the VX-200 experimental test configuration with recent improvements to the system. It is fully operational with a power capability of 200 kW and pulse lengths limited by the vacuum facility and thermal management. The performance of the rocket from DC electrical power to effective jet power is well established. The DC to RF conversion efficiency is 95±1% and the thruster efficiency (RF to jet power) is 72 ± 9% at 200 kW of RF power and an I_{sp} of 4900 ± 300 seconds. A thrust of 5.8 ± 0.4 N has been measured.

For the first time, we have collected a detailed map of the exhaust plume with a low background neutral pressure ($< 10^{-5}$ torr). We compared the expansion of the plasma plume with the magnetic field to 2.4 m downstream of the thruster exit plane. This shows compelling evidence that the plasma does not follow the magnetic field lines and remains mostly axially directed with high ICH power. This is shown by comparing the plasma flux to the magnetic flux expansion. The magnetic flux clearly expands radially faster than the high energy plasma flux, well outside the error of measurement.

We have introduced a proposed project to install an Electric Propulsion and Power Platform, named *Aurora*, mounted externally on the International Space Station. This asset would demonstrate the function of a VASIMR VF-200 device in space while potentially also offering power and data resources to other devices that could benefit from testing in space where they may be accessed and retrieved.

Acknowledgments

The authors would like to thank the support of MEI Technologies, Inc.

References

[1]Chang Diaz, F. R., *Scientific American* **283** (2000) 72.

[2]Glover, T. W., Chang-Díaz, F. R., et al.: "Principal VASIMR Results and Present Objectives," *Space Technology and Applications International Forum*, Albuquerque, NM, 2005.

[3]Boswell, R. W. and Chen, F. F.: *IEEE Transactions of Plasma Science* **25** (1997) 1229.

[4]Chen, F. F. and Boswell, R. W.: *IEEE Transactions of Plasma Science* **25** (1997) 1245.

[5]Arefiev, A. V. and Breizman, B. N.: *Physics of Plasmas* **11** (2004).

[6]Squire, J. P., Chang Diaz, F. R., et al. (2008). "VASIMR Performance Measurements at Powers Exceeding 50 kW and Lunar Robotic Mission Applications." *International Interdisciplinary Symposium on Gaseous and Liquid Plasmas*, Sep 5-6 2008, Akiu/Sendai, Japan.

[7]Cassady, L. D., Longmier, B. W., Olsen, C. S., Ballenger, M. G., McCaskill, G. E., Ilin, A. V., Carter, M. D., Glover, T. W., Squire, J. P. , Chang Díaz, F. R., "VASIMR Performance Results," AIAA Paper 2010-6772, *46th AIAA/ASME/SAE/ASEE Joint Propulsion Conference & Exhibit*, Nashville, TN, 25-28 July, 2010.

[8]Bering III, E.A., Chang Díaz,F.R., Squire,J.P., Glover, T.W., Carter, M.D., McCaskill, G.E., Longmier, B.W., Brukardt, M.S., Chancery, W.J., Jacobson, V.T., "Observations of single-pass ion cyclotron heating in a trans-sonic flowing plasma," *Physics of Plasmas* 17, 043509, 2010.

[9]Squire, J. P., Chang-Díaz, F. R., Carter, M. D., Cassady, L. D., Chancery, W. J., Glover, T. W., Jacobson, V. J., McCaskill, G. E., Bengtson, R. D., Bering, E. A., Deline, C. D.: "High Power VASIMR Experiments using Deuterium, Neon and Argon", *30th International Electric Propulsion Conference*, IEPC-2007-181, Sept. 2007.

[10]Squire, J. P., Cassady, L. D., Chang Díaz, F. R., Carter, M. D., Glover, T. G., A.V. Ilin, Longmier, B. W., McCaskill, G.E., Olsen, C. S. and Bering, E. A., presented at the *31st International Electric Propulsion Conference*, Ann Arbor, Michigan (2009)

[11]Bering, E. A., Longmier, B. W., Ballenger, M. G., Olsen, C. S., Squire, J. P., Chang-Díaz, F. R., "Performance Studies of the VASIMR® VX-200". *49th AIAA Aerospace Sciences Meeting and Exhibit*. Orlando, FL. February, 2011.

[12]Stix, T. H.: Waves in Plasmas, American Institute of Physics, New-York NY, 1992.

[13]Longmier, B. W., Reid, B. M., Gallimore, A. D., Chang-Díaz, F. R., Squire, J. P., Glover, T. W., Chavers, D. G., Bering, E. A., "Validating a Plasma Momentum Flux Sensor to an Inverted Pendulum Thrust Stand, *Journal of Propulsion and Power*," Vol. 25, No. 3, 2009, pp. 746-752.

[14] Longmier, B. W., Cassady, L. D., Ballenger, M. G., Carter, M. D., Chang Díaz, F. R., Glover, T. W., Ilin, A. V., McCaskill, G. E., Olsen, C. S., Squire, J. P., and Bering, III, E.A., VX-200 Magnetoplasma Thruster Performance Results Exceeding Fifty-Percent Thruster Efficiency, *JOURNAL OF PROPULSION AND POWER*, Vol. 27, No. 4, July–August, 2011.

[15]Longmier, B. W., *32nd International Electric Propulsion Conference*, Wiesbaden, Germany, paper number 156.

[16] Gesto, F. N., Blackwell, B. D., Charles, C., and Boswell, R. W., *Journal of Propulsion & Power* **22**, 24 2006.

[17] Deline, C. A., Bengston, R. D., Breizman, B. N., Tushentsov, M. R., Jones, J. E., Chavers, D. G., Dobson, C. C., and Schuettpelz, B. M., *Physics of Plasmas*, 16, 033502, 2009.

[18] Del Valle Gamboa, J. I., *32nd International Electric Propulsion Conference*, Wiesbaden, Germany, paper number 151.